Journal of Global Optimization, 11, 69–82 (1997)

Growth of Nanophase Clusters and Potential Energy Minima: Hysteresis, Oscillations, and Phase Transitions

D.G. VLACHOS*
Department of Chemical Engineering, University of Massachusetts, Amherst, Massachusetts 01003.
Email: vlachos@@ecs.umass.edu

Abstract. The structures of small Lennard-Jones clusters (local and global minima) in the range $n = 30 - 55$ atoms are investigated during growth by random atom deposition using Monte Carlo simulations. The cohesive energy, average coordination number, and bond angles are calculated at different temperatures and deposition rates. Deposition conditions which favor thermodynamically stable (global minima) and metastable (local minima) are determined. We have found that the transition from polyicosahedral to quasicrystalline structures during cluster growth exhibits hysteresis at low temperatures. A minimum critical size is required for the evolution of the quasicrystalline family, which is larger than the one predicted by thermodynamics and depends on the temperature and the deposition rate. Oscillations between polyicosahedral and quasicrystalline structures occur at high temperatures in a certain size regime. Implications for the applicability of global optimization techniques to cluster structure determination are also discussed.

Keywords: Optimization, simulated annealing, molecular structures

1. Introduction

The structures of small Lennard-Jones (LJ) clusters at 0 K have been extensively studied (Briant and Burton, 1975; Farges, et al., 1986; Farges, et al., 1983; Hoare, 1979; Hoare and Pal, 1971; McGinty, 1973; Northby, 1987; Raonlt, et al., 1989; Wille, 1987). Hoare and Pal (1971) proposed the earliest comprehensive study on the structures of small Ar clusters in the range $n < 56$ atoms. Their model was based on several initial seed structures of different symmetry. Single atoms were successively added at 0 K to the seed structures resulting in many locally stable minima (isomers). Noncrystalline clusters were found to be more stable than face-centered cubic structures for small cluster sizes.

Farges et al. performed molecular dynamics (MD) for $n < 51$, and the structures formed were termed polyicosahedral (PIC) (Farges, et al., 1986). These structures consisted of interpenetrating icosahedra and exhibit only pentagonal rings (111 microfacets). Northby (1987) used a lattice-based search optimization procedure to find the minimum energy structures of $n = 13 - 147$, which were considered to be tightly bounded multilayer icosahedra. We investigated LJ clusters in the range $n < 35$ and found that there exists an abrupt phase transition from $n = 30$ to

*THIS WORK WAS SUPPORTED IN PART BY NSF UNDER GRANT NUMBER CTS-9410994 AND THE ENGINEERING COMPUTING SERVICES OF THE UNIVERSITY OF MASSACHUSETTS.

$n = 31$ (Vlachos, et al., 1992). At low temperatures and above this size, qnasicrystalline (QC) structures become thermodynamically more favorable than PIC structures. QC clusters exhibit both pentagonal and square rings. More recently, a global energy minimization scheme has been proposed (Maranas and Floudas, 1992; Maranas and Floudas, 1994), and the role of quenching in LJ cluster morphology has been studied (Zacharias and Vlachos, 1996).

Even though structures of clusters have received considerable attention, less is known about growth of clusters at finite temperatures where the free energy must be known. Furthermore, growth is an out of equilibrium process, and the resulting structures may not correspond to global minima of the potential energy surface. As a result, even though global optimization techniques are important, they may be not practical for predicting physical situations.

Here we propose a microscopic model to investigate gas-phase growth of LJ clusters in the range $n = 30 - 55$ atoms using MC simulations. We examine the roles of kinetics and thermodynamics on the morphology of clusters as functions of temperature and deposition rate. These studies can reveal how far-from-equilibrium growth can proceed in order for equilibrium structures (global minima) to form. In particular, the phase transition from PIC to QC cluster is examined. This phase transition is especially interesting because it may exhibit generic features of phase transitions taking place when symmetry changes occur during growth.

2. Interatomic potential and structural properties

The Metropolis walk MC method (Metropolis, et al., 1953) is implemented in our simulations (Zacharias and Vlachos, 1996). Typically, each atom is moved by a random displacement in three dimensions, and the energy change associated with the attempt is calculated. If the energy of the system is lowered, the step is accepted; otherwise the trial is accepted with probability given by a Boltzmann factor. The maximum displacement is adjusted during the simulations so that an acceptance ratio of 0.3 is maintained. One Monte Carlo step (MCS) consists of sampling all atoms once on the average.

For a cluster of n atoms, the cohesive energy E, using the pairwise LJ potential, is

$$E = 4\epsilon \sum_{i<j=1}^{n} [(\sigma/r_{ij})^{12} - (\sigma/r_{ij})^{6}], \tag{1}$$

where r_{ij} is the distance between atoms i and j. Here dimensionless temperature is used, i.e., $T^{*} = kT/\epsilon$. The full range of the LJ potential is employed. Two atoms are considered to be first nearest neighbors when their distance is less than $r_c = 1.3\sigma$. This distance is approximately equal to the arithmetic mean of the distances of the first and the second nearest neighbors in bulk face-centered cubic materials.

Let nn_i be the number of nearest neighbors of atom i in the cluster, i.e., the coordination of atom i. The average coordination number CN of a cluster is defined as

$$CN = \sum_{i-1}^{n} nn_i/n \tag{2}$$

and indicates the compactness of a cluster.

The probabilities of various bond angles are also used to identify clusters which may be close in energy but different in structure (Vlachos, et al., 1992). p_{90} and p_{108} are defined as the fractions of the total number of bond angles in the cluster with 90^o and 108^o angles, respectively. PIC clusters exhibit pentagonal rings only, manifested by a nonzero p_{108}, but no squares ($p_{90} = 0$). QC clusters exhibit both pentagonal and square rings, manifested by 90^o and 108^o bond angles. Crystalline clusters do not exhibit any fivefold rings ($p_{108} = 0$). Thus, the bond angle probabilities are an efficient way to observe solid-to-solid phase transitions between cluster families of different symmetry.

Fig. 1 shows the probabilities of 90^o and 108^o bond angles, and the average coordination number of the most stable LJ clusters in the range $n = 2 - 55$ at $T^* = 1.610^{-4}$. The data is taken from our simulated annealing calculations. These minimum energy structures are in agreement with Northby's data (Northby, 1987) and many of them are more stable than those found in the pioneer work of Hoare and Pal (1971). In particular, sizes found by Hoare and Pal which differ from ours are: $n = 17, 22, 23, 24, 28, 30 - 54$ (the minimum energy of clusters of $n = 47 - 53$ was not reported by Hoare and Pal). The abrupt phase transition from $n = 30$ to $n = 31$ was not found in the original work of Hoare and Pal. This phase transition from $n = 30$ (PIC) to $n = 31(QC)$ is manifested in Fig. 1a by an increase in p_{90} and a decrease in p_{108}. In addition, a discontinuous decrease in CN occurs at this size as shown in Fig. 1b.

3. Growth model

For most of the growth simulations, the most stable $n = 30$ isomer (global minimum) is used as an initial structure. This cluster is maintained at some specified temperature and is equilibrated for a period of time (a certain number of MCS) before a new atom is added. First the center of mass of the cluster is calculated which is then used as the center of a sphere with a radius equal to the farthest distance between the center of mass and any atom in the cluster plus a shifting distance. This distance is typically equal to r_c. A shorter shifting distance is adopted for fast growth where deposited atoms do not have sufficient time for incorporation into the cluster. Atom deposition occurs at a random position on the surface of this sphere, which is a reasonable model when transport in the gas phase is not rate limiting. The time between successive atom additions determines the deposition rate in units of atoms/MCS. Even though MCS are not directly related to real time, a smaller

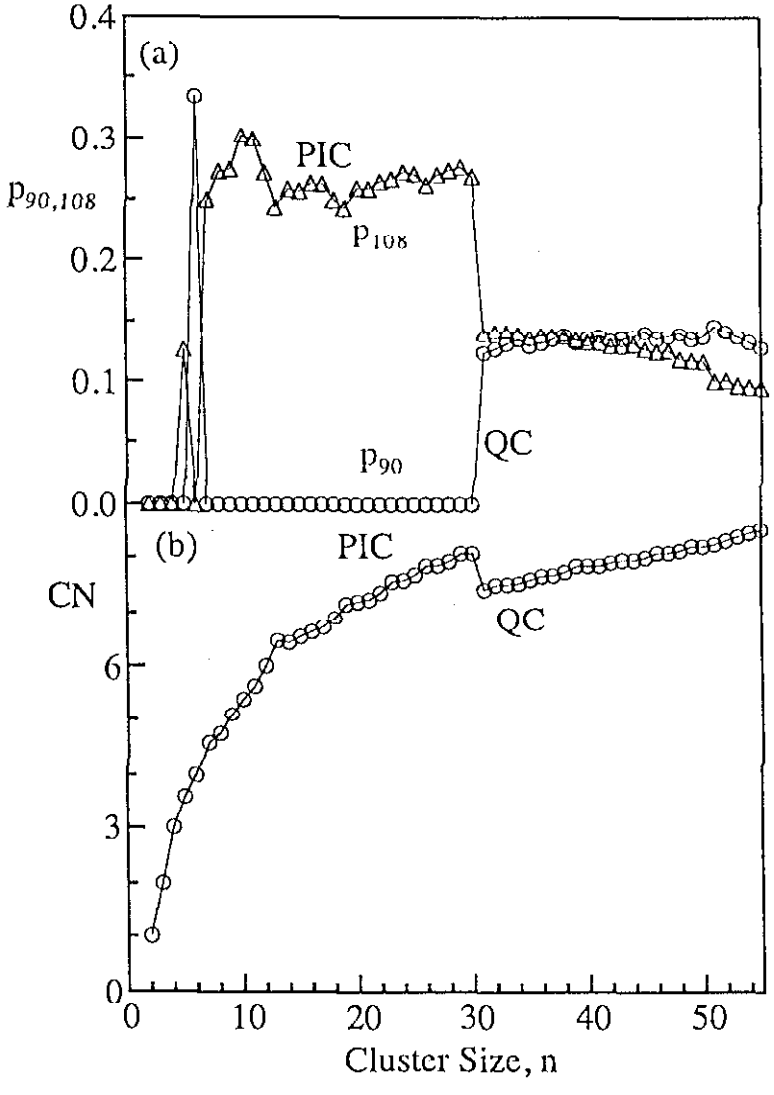

Figure 1. Structural properties of the most stable (global minima) LJ clusters in the size regime of $n = 2 - 55$. Panel a shows the probabilities of 90° and 108° bond angles versus cluster size n. A transition from QC to PIC structures occurs from 30 to 31 atoms. Panel b shows the average coordination number CN versus n. A substantial decrease from $n = 30$ to $n = 31$ occurs. QC clusters are less compact than PIC clusters.

number of MCS can make the system move away from equilibrium. A cluster grows due to atom incorporation and can equilibrate between successive atom depositions

due to free energy minimization. Growth proceeds until a specified maximum size is reached.

Simulations have been performed in the desorption-limited regime, i.e., the growth rate is much faster than desorption so that desorption events do not occur at these time scales and temperatures. Even though the overall growth process proceeds in an out-of-equilibrium state, local equilibrium at the growing cluster can be established by surface diffusion or isomerization (synergetic effects of many atoms). Growth is modeled as an isothermal process during which rapid removal of the adsorption energy occurs either by gas-phase collisions between the cluster and an inert atmosphere or by surface energy transport for supported clusters.

Instantaneous quenching of clusters to low temperatures is important in determining cluster isomers (minima) visited by a cluster at high temperatures. In our MC simulations, instantaneous quenching down to $T^* = 1.610^{-4}$ has been periodically adopted to detect cluster isomerization during growth. In most of the following plots, twenty sampling points from such quenching runs are typically shown for each cluster size.

The simulations have been performed on DEC 3000/600 AXP workstations. For a growth simulation with a deposition rate of 10^{-7} atoms/MCS, almost ten days of CPU time are required for cluster growth from $n = 30$ to $n = 55$ atoms, and many of these runs are needed.

4. Hysteresis during growth

As mentioned above, for $n > 30$, QC isomers are thermodynamically more stable at low temperatures, whereas PIC structures are favorable at sufficiently high temperatures (Vlachos, et al., 1992). Fig. 2 shows p_{90} and p_{108} for the growth from $n = 30$ to $n = 55$ atoms at $T^* = 0.07$ with a deposition rate of 10^{-6} atoms/MCS (solid lines). A phase transition from PIC to QC structures occurs at n=36 atoms where an abrupt increase in p_{90} and a decrease in p_{108} occur.

Our simulations indicate a delay in cluster morphology (local minima form between $n = 31$ and $n = 35$). The most stable family (global minima) forms at a larger cluster size. This delay (hysteresis) is analogous to superheating of materials when temperature is the control variable. Such a behavior is found for the first time in computer simulations.

The initially PIC cluster transforms into a QC structure in a short time after the deposition of the new atom. This transition is associated with a substantial decrease in the number of pentagonal rings. In particular, the $n = 35$ cluster is a PIC local minimum energy isomer. When an atom is added, a $n = 36$ PIC cluster is first formed with only pentagonal rings. Synergetic atom rearrangements result in a transition over a saddle point in the potential hypersurface that leads to a $n = 36$ QC cluster.

Besides these growth simulations, we should note that slow quenching also fails to form the thermodynamically most stable structures in the same size regime (Zacharias and Vlachos, 1996). In addition, although the experimentally observed

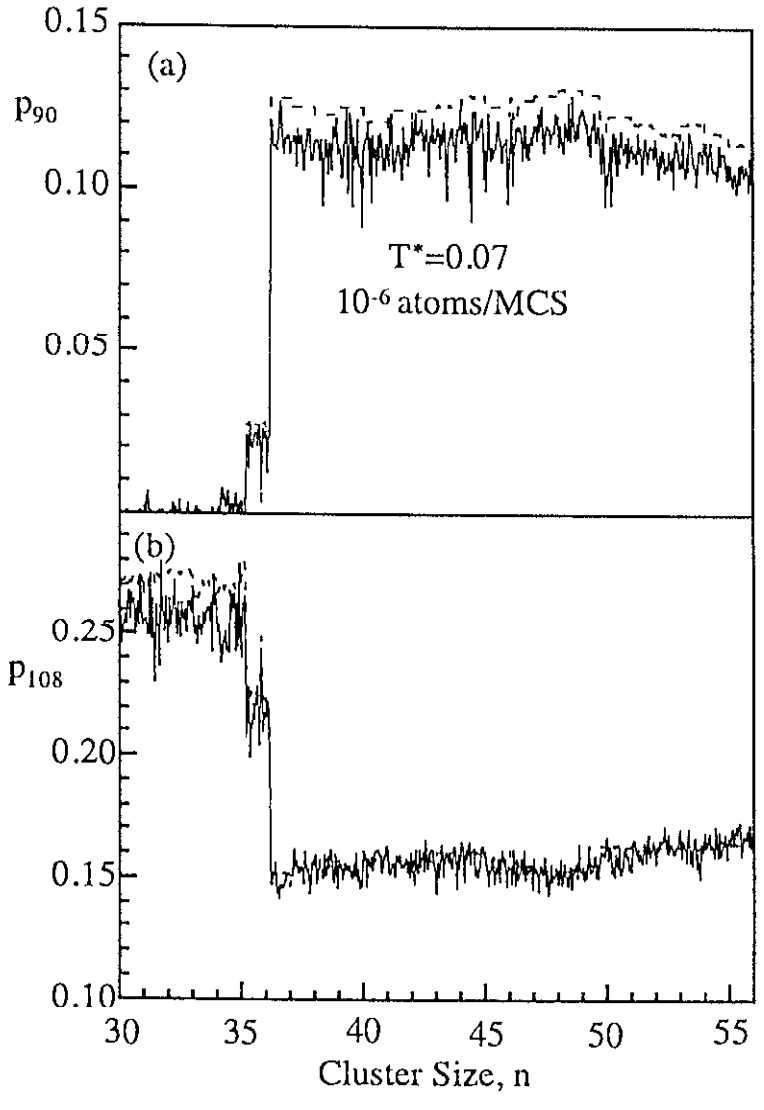

Figure 2. Panels a and b show p_{90} and p_{108} versus cluster size n for growth at $T^* = 0.07$. The solid and dotted lines indicate data before and after quenching, respectively. A phase transition from PIC to QC clusters occurs at $n = 36$.

ionized, magic number Ar clusters (Harris, et al., 1984) coincide with the local maxima in the sublimation energy shown in Fig. 1, discrepancies are observed for

$n = 34$. This indicates that a nucleation barrier may exist in the formation of (100) square microfacets in QC clusters in the range $n = 31$ to $n = 35$.

The dashed lines in Fig. 2 show the corresponding data after the snapshots have been quenched to $T^* = 1.610^{-4}$. Qnenching restores some pentagonal and square rings smeared by thermal fluctuations. However, most structural features coincide before and after quenching. In the rest of the plots in this paper, only data after quenching is shown. p_{90} and p_{108} provide often complementary information, i.e., when one increases, the other one decreases. Thus, only p_{90} is shown below.

5. Oscillations in cluster morphology

Fig. 3 shows p_{90} versus cluster size at $T^* = 0.17$. At this temperature, the transition from PIC to QC isomers is not abrupt as happened in Fig. 2. Instead, when growth is slow, interconversions between PIC and QC clusters (minima of the two families) are observed which result in oscillations of structural properties. These oscillations have been observed in all runs of slow growth. Oscillations between different families of Au clusters have been observed experimentally upon heating (Ajayan and Marks, 1989).

Coexistence of PIC and QC clusters is found between a minimum and a maximum critical size. In this coexistence regime, the nucleation barriers separating the PIC and QC families are presumably not too high compared to the thermal energy so that oscillations are observed. These two critical sizes depend on the temperature and the growth rate. When growth is fast, the characteristic time for oscillations is, on the average, longer than the time for atom addition, and this oscillatory behavior disappears (only one family of isomers is observed). Thus, oscillations are favored near thermodynamic equilibrium.

6. Effects of deposition rate and temperature

Here we first examine the effect of deposition rate on the morphology of clusters formed. p_{90} is shown in Fig. 4 at $T^* = 0.1$ for various deposition rates indicated. The square markers are the corresponding values for the thermodynamically most stable structures (global minima) at $T^* = 1.610^{-4}$ which are used as a reference for comparison.

The appearance of QC structures is indicated by an abrupt increase in p_{90} to a non-zero value at a minimum critical size. For n greater than this critical size, the QC family dominates. This critical size is $n = 44$, 39, and 37 for 10^{-5}, 10^{-6} and 10^{-7} atoms/MCS, respectively. For sufficiently fast growth, the phase transition fails to happen in the size regime of $n = 30 - 55$. Before the QC family has dominated, there can be occasionally a trace of 90^o bond angles found in the structures. For sufficiently slow growth, the QC cluster can isomerize to PIC cluster and back again as shown in Fig. 4 with a deposition rate of 10^{-7} atoms/MCS.

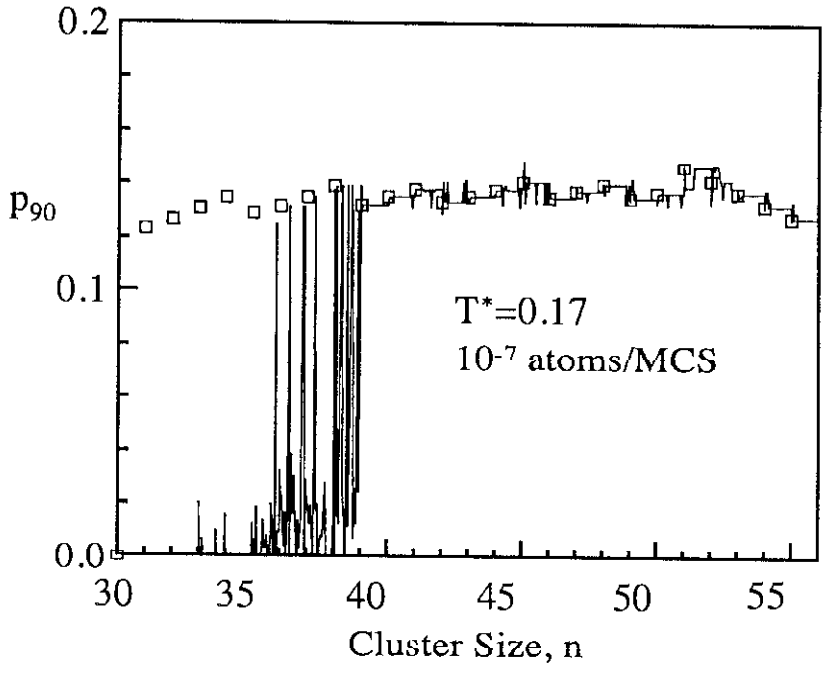

Figure 3. Oscillations in cluster morphology at $T^* = 0.17$. When growth is slow, interconversions between PIC and QC clusters are observed in a certain size regime.

Comparison of the results at 10^{-6} atoms/MCS and 10^{-7} atoms/MCS in Figs. 2-4 indicates that below a certain deposition rate, the minimum critical size does not depend on the deposition rate, at least within the accuracy of the simulations. Thus, the hysteresis is probably caused by a nucleation barrier in the formation of (100) microfacets rather than the irreversibility of the growth process.

Note that the critical size depends significantly on the growth rate when deposition is fast. For high deposition rates, isomerization times may be long compared to growth times, and thus, there seems to be no sufficient time for a cluster to isomerize to form a global minimum. As a result, a cluster is trapped into a local minimum PIC structure and oscillations are not observed. Under such conditions, global optimization techniques predict structures which probably do not form experimentally.

We emphasize that the most stable clusters (global minima) can form in our simulations at larger sizes ($n > 35$) for slow deposition. Since typical time scales of long molecular simulations (e.g., MD simulations) are of the order of nanoseconds, the slowest growth rates in our simulations are much higher than the corresponding growth rates of practical applications. Thus even at far-from-equilibrium conditions, thermodynamics dominates and results in formation of global minima, at

least for these sizes. This indicates that deterministic optimization techniques can be used for such systems when phase transitions are not involved.

The probability of forming the global minimum energy structures during growth increases as the deposition rate decreases. In general, slow deposition leads to lower energy structures at each size. For example, at $T^* = 0.17$, all isomers formed during growth were local energy minima for 10^{-4} atoms/MCS. For 10^{-6} atoms/MCS, global energy minima were found in the range $n = 38$–45, and for 10^{-7} atoms/MCS, the most stable isomers dominated in the size range from $n = 36$ to $n = 55$. Thus the slower the deposition, the more probable that global optimization techniques provide the correct structure.

Fig. 4 indicates that a critical deposition rate is required for the appearance of QC clusters. When the deposition rate is too high compared to the isomerization rates, the QC family fails to form and metastable isomers are found. The questions that arise are whether QC isomers form at larger sizes and what are the structures of fast grown clusters. When deposition is fast, amorphous clusters are expected. The distinction between metastable and amorphous clusters is not always clear. The microamorphous state of structures upon fast cooling has been recently discussed by Berry and co-workers for alkali halide clusters (Rose and Berry, 1993).

In order to examine the deposition rates required for the occurrence of the QC family, simulations of fast growth have been carried out at various temperatures. These results are summarized in Fig. 5. The points shown in Fig. 5 for deposition rates larger than 10^{-6} atoms/MCS are averages over 40–50 runs. This kind of phase diagram should be considered only semi-quantitatively because of the uncertainty in determining the critical size, especially for fast growth and at low temperatures. The minimum critical size decreases considerably as the deposition rate decreases from high values and approaches a plateau for slow growth indicating the existence of a nucleation barrier. The increase in the critical size with increasing deposition rate is probably due to the fact that for fast growth, there is no sufficient time for the phase transition to occur. As atoms are deposited, a core cluster has sufficient time to isomerize to a QC structure.

Clusters grown slowly exhibit well-defined peaks in the angular distribution function (ADF) at 60^o, 90^o, and 108^o, corresponding to characteristic structures, i.e., (111) microtriangles, (100) square rings, and pentagonal rings. As an example, Fig. 6a shows the ADF of the $n = 55$ MacKay icosahedron formed at $T^* = 0.13$ with a deposition rate of 10^{-7} atoms/MCS. This is the most stable known structure of $n = 55$ at low temperatures. Fig. 6b shows the ADF of a $n = 55$ cluster grown from a dimmer at a fast deposition rate of 10^{-2} atoms/MCS. This is a much less compact structure without any crystallinity ($p_{90} = 0$). Even for computationally fast growth, the ADF exhibits peaks characteristic of metastable clusters. Deposition started from a dimmer at a rate of 1 atom/MCS resulted in a random agglomeration of 55 atoms with a Gaussian-like ADF as shown in Fig. 6c. This is reminiscent of ballistic deposition of atoms. Compared with the MacKay icosahedron, the $n = 55$ cluster formed at 10^{-2} atoms/MCS does not display either 90^o or 150^o, and the fast grown cluster at 1 atom/MCS shows a completely smeared ADF. Fast depo-

sition does not provide sufficient time for equilibration, and thus, it results in less compact structures in which added atoms are randomly deposited around an initial nucleus.

Regarding the effect of temperature on the formation of the most stable structures, at low temperatures clusters formed are less compact than the global energy minima after the phase transition has occurred. As the temperature increases, the structures grown coincide often with the most stable clusters because clusters can jump over nucleation barriers separating different cluster families. As a result, the most stable isomers are found more frequently at sufficiently low growth rates, e.g., for $n = 36 - 55$ atoms at $T^* = 0.17$ but only for $n = 39$ and 40 at $T^* = 0.10$.

7. Conclusions

We have simulated the growth of LJ clusters by atom deposition from $n = 30$ to $n = 55$ atoms. We have found that there exists hysteresis in the transition from polyicosahedral (PIC) to quasicrystalline (QC) clusters, which is affected by temperature and growth rate. Although QC clusters are thermodynamically favored for $n > 30$ atoms at low temperatures (global minima), QC configurations are not formed in the range $n = 31-35$ even at low (computationally) deposition rates. This hysteresis in cluster size is probably caused by a large nucleation barrier between the PIC and QC families. Fast growth can delay the size at which QC clusters appear. Oscillations in cluster morphology occur in an intermediate size regime at high temperatures where the thermal energy is sufficient for interconversions between the two cluster families.

Even though growth on the computer is very fast, we have been able to find that the most stable LJ clusters form in the range $n = 36-55$. Thus global optimization techniques are useful in predicting the structures (global minima) of clusters at low temperatures for relatively small sizes except when abrupt changes in structure occur (e.g, $n = 31 - 35$).

8. References

P. M. Ajayan and L. D. Marks, *Experimental evidence for quasimelting in small particles*, Phys. Rev. Letters **63** (1989), 279-282.

C. L. Briant and J. J. Burton, *Molecular dynamics study of the structure and thermodynamic properties of argon microclusters*, J. Chem. Phys. **63** (1975), 2045-2058.

J. Farges, M. F. De Feraudy, B. Raoult, and G. Torchet, *Noncrystalline structure of argon clusters. II. Multilayer icosahedral structure of Ar_N clusters $50 < N < 750$*, J. Chem. Phys. **84** (1986), 3491-3501.

J. Farges, M. F. Feraudy, B. Raoult, and G. Torchet, *Noncrystalline structure of argon clusters. 1. Polyicosahedral structure of Ar_N clusters, $20 < N < 50$*, J. Chem. Phys. **78** (1983), 5067-5080.

I. A. Harris, R. S. Kidwell, and J. A. Northby, *Structure of charged argon clusters formed in a free jet expansion*, Phys. Rev. Letters **53** (1984), 2390-2393.

M. R. Hoare, *Structure and dynamics of simple microclusters*, Adv. Chem. Phys. **40** (1979), 49.

M. R. Hoare and P. Pal, *Physical cluster mechanics: Statics and energy surfaces for monatomic systems*, Adv. Phys. **20** (1971), 161-196.

C. D. Maranas and C. A. Floudas, *A global optimization approach for Lennard-Jones microclusters*, J. Chem. Phys. **97** (1992), 7667-7678.

C. D. Maranas and C. A. Floudas, *A deterministic global optimization approach for molecular structure determination*, J. Chem. Phys. **100** (1994), 1247-1261.

D. J. McGinty, *Molecular dynamics studies of the properties of small clusters of argon atoms*, J. Chem. Phys. **58** (1973), 4733-4742.

N. Metropolis, A. W. Rosenbluth, M. N. Rosenbluth, A. H. Teller, aud E. Teller, *Equation of state calculations by fast computing machines*, J. Chem. Phys. **21** (1953), 1087-1092.

J. A. Northby, *Structure and binding of Lennard-Jones clusters:* $13 < N < 147$, J. Chem. Phys. **87** (1987), 6166-6177.

B. Raoult, J. Farges, M. F. De Feraudy, and G. Torchet, *Comparison between icosahedral, decahedral and crystalline Lennard-Jones models containing 500 to 6000 atoms*, Phil. Magazine B **60** (1989), 881-906.

J. P. Rose and R. S. Berry, $(KCl)_{32}$ *and the possibilities for glassy clusters*, J. Chem. Phys. **98** (1993), 3262-3274.

D. G. Vlachos, L. D. Schmidt, and R. Aris, *Structures of small metal clusters: I Low temperature behavior*, J. Chem. Phys. **96** (1992), 6880-6890.

D. G. Vlachos, L. D. Schmidt, and R. Aris, *Structures of small metal clusters: II Phase transitions and isomerization*, J. Chem. Phys. **96** (1992), 6891-6901.

L. T. Wille, *Minimum-energy configurations of atomic clusters: New results obtained by simulated annealing*, Chem. Phys. Letters **133** (1987), 405-410.

M. M. Zacharias and D. G. Vlachos, *Simulated annealing calculations for optimization of nanoclusters: The roles of quenching, nucleation, and isomerization in cluster morphology*, in Global minimization of nonconvex energy functions: Molecular conformation and protein folding, edited by P. M. Pardalos, D. Shalloway, and G. Xue, Vol. 23, (AMS, 1996), p. 251-271.

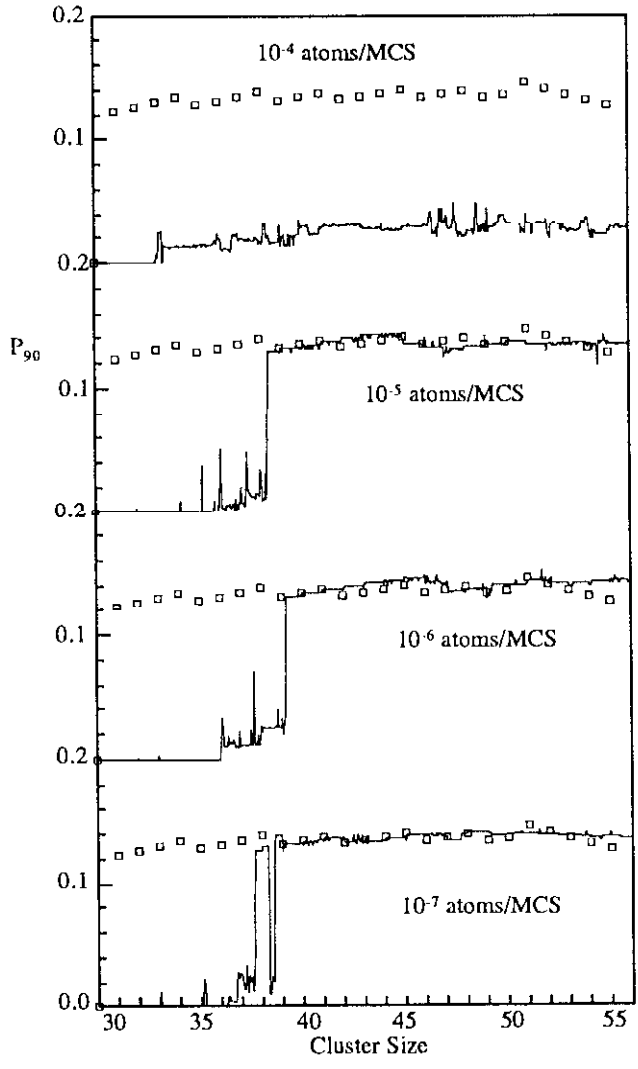

Figure 4. Effect of deposition rate on p_{90} for growth at $T^* = 0.10$. When the deposition rate is too fast (10^{-4} atoms/MCS), the phase transition can happen at a size larger than $n = 55$. The average critical cluster size for the phase transition decreases as the deposition rate decreases and is affected slightly by the deposition rate for sufficiently slow growth. The square markers correspond to the most stable (global minima) LJ clusters.

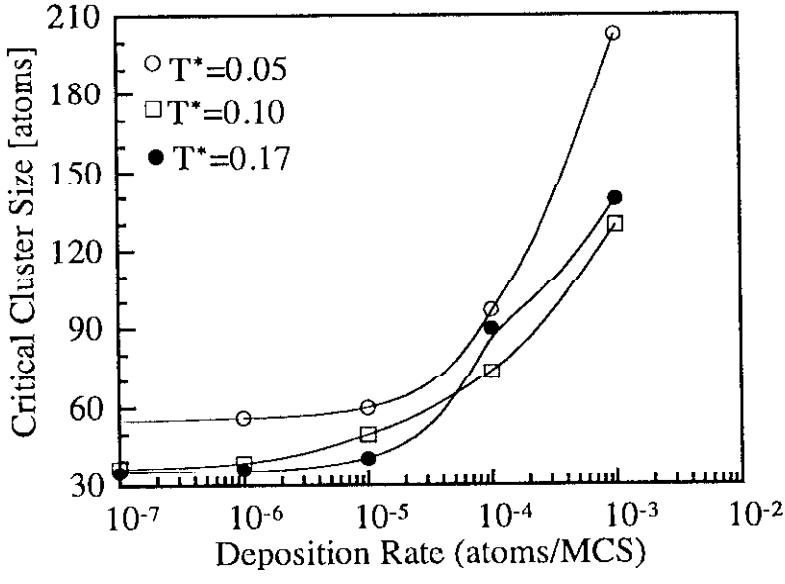

Figure 5. Effect of deposition rate on the minimum critical size at various temperatures. The minimum critical size drops sharply as the deposition rate decreases and approaches a plateau for sufficiently low growth rates.

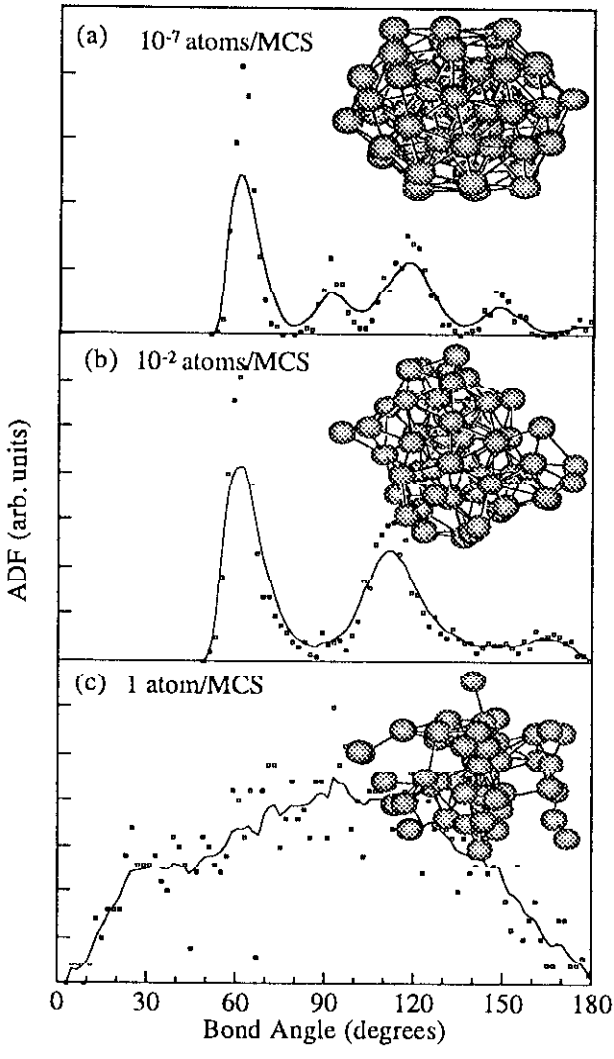

Figure 6. ADF for the $n = 55$ cluster grown at different deposition rates at $T^* = 0.13$. Panel a shows the most stable $n = 55$ MacKay icosahedron grown at 10^{-7} atoms/MCS from the $n = 30$ most stable nucleus. Well-defined peaks denoting characteristic microfacets are found. Panels b and c show the structures of fast grown clusters starting from the $n = 2$ dimmer as a nucleus. Less compact structures are formed for fast growth. The points are obtained from simulations and the lines just connect the points.